CHEMISTRY OF MATERIALS

ARTICLE

pubs.acs.org/cm

Synthesis and Materials Properties of Sn/P-Doped Ge on Si(100): Photoluminescence and Prototype Devices

Richard T. Beeler,[†] Gordon J. Grzybowski,[†] Radek Roucka,[†] Liying Jiang,[‡] Jay Mathews,[‡] David J. Smith,[‡] José Menéndez,[‡] Andrew V. G. Chizmeshya,[†] and John Kouvetakis[*,†]

[†]Department of Chemistry and Biochemistry, Arizona State University, Tempe, Arizona 85287-1604, United States

[‡]Department of Physics, Arizona State University, Tempe, Arizona 85287-1504, United States

ABSTRACT: We report the fabrication of a new class of Sn/P-doped Ge-like materials with high quality optical, structural, and device properties. A flux of Ge_2H_6 with trace amounts of SnD_4 is used to deposit thick Sn-doped Ge films via chemical vapor deposition (CVD) at low temperatures (~390−370 °C) directly on Si(100) substrates. The presence of Sn in the gas mixture alters the standard Ge growth mechanism (Stranski−Krastanov) to yield atomically smooth layers with minimal threading defects at growth rates as high as 15−30 nm/min. The films, dubbed "quasi-Ge", contain $\sim 10^{19}$ cm^{-3} Sn "impurities", which do not produce any measurable shift in the lattice constant or emission wavelength. This new method represents a low-cost, high-performance alternative to the standard CVD approaches to grow high-quality Ge-on-Si for optoelectronic applications. In this regard, the optical quality of the materials is corroborated by studying photoluminescence (PL) of both intrinsic samples and *n*-type analogues doped well above 10^{19} atoms cm^{-3}, using the single-source $P(GeH_3)_3$. Heavy *n*-doping significantly enhances the PL intensity, allowing the observation of distinct indirect and direct gap peaks. The device quality of the material was evaluated by fabricating prototype heterostructure photodetectors in *n-i-p* geometry. These are found to exhibit significantly higher responsivities than pure Ge *p-i-n* analogues and dark current densities comparable to the state of the art.

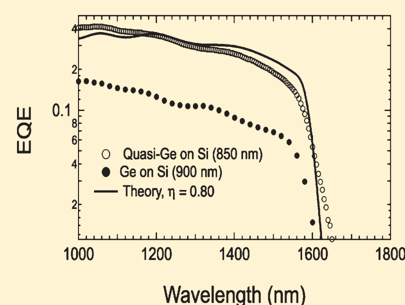

KEYWORDS: IR optoelectonics, photodetectors, Ge, GeSn alloys, Sn-doped Ge

I. INTRODUCTION

The epitaxial growth of high-quality Ge on Si has long been recognized as a critical milestone in the quest to extend the Si functionality for logical and optoelectronic applications. Different approaches have been proposed, from compositionally graded $Si_{1-x}Ge_x$ buffer layers[1,2] to the deposition of low-temperature initiation layers.[3,4] Recently, Wistey and co-workers[5] introduced an alternative low-temperature ($T < 400$ °C) method based on low-pressure chemical vapor deposition (CVD) reactions of $CH_2(GeH_3)_2$ metallorganic additives with large amounts of Ge_2H_6. This approach yields thick, device-quality films with extremely low dislocation densities ($<10^5/cm^2$) and atomically flat surfaces. However, the single-wafer nature of this method casts doubt regarding its industrial viability, particularly for photovoltaic applications where the main driver for the development of Ge-on-Si technologies is the very high cost of Ge substrates. Accordingly, in this paper, we discuss a CVD approach to the epitaxial growth of Ge on Si substrates that enables the fabrication of a high-quality material on multiple substrates during a single run, at industrial scale growth rates approaching 30 nm/min. Our method is an extrapolation of the approach that we have previously used to grow $Ge_{1-y}Sn_y$ alloys, and, more recently, Sn-doped Ge with enhanced absorption at 1550 nm. It was originally introduced by Bauer et al.,[6] who used mixtures of digermane (Ge_2H_6) and deuterated stannane (SnD_4) to grow $Ge_{1-y}Sn_y$ alloys with $0.01 < y < 0.20$. A crucial finding was that the presence of SnD_4 completely changes the growth mode from Stranski−Krastanov (SK) to Frank−van der Merwe (FM), i.e., from layer-plus-island to layer-by-layer. The precise role of SnD_4 remains unclear, but it seems likely that it affects the lateral atomic migration at the same time that it promotes the elimination of H_2 from the growth front. The resulting alloy films were found to possess atomically flat surfaces and were virtually devoid of threading dislocations.

Given the dual role of SnD_4 as a supplier of Sn atoms and facilitator of the FM growth mode, the question arises as to what minimum amount is needed to maintain layer-by-layer growth. Very recently, we showed that it was possible to obtain high-quality films with Sn doping in the 10^{20} cm^{-3} range. In particular, we studied in detail a *p-i-n* device with a $Ge_{0.997}Sn_{0.003}$ intrinsic layer in which the absorption edge was slightly displaced with respect to pure Ge.[7] In the present paper, we discuss Sn doping levels of $\sim 10^{19}$ cm^{-3}, for which no measurable difference is seen between the optical properties of the doped material and that of pure Ge. These extremely diluted alloys are dubbed "quasi-Ge".

In Section II of the paper, we discuss the growth of quasi-Ge and its structural properties, and describe the fabrication of P-doped counterparts containing similar Sn levels. The photoluminescence (PL) properties of the material are discussed in

Received: June 10, 2011
Revised: August 22, 2011
Published: September 21, 2011

 © 2011 American Chemical Society

Section III, where we first demonstrate that minute levels of Sn (0.05%−0.15%) have negligible effect on the emission wavelength of intrinsic materials, compared to that of a pure Ge reference sample treated under identical conditions. We show that heavy *n*-type doping significantly enhances the PL intensity while leading to spectra in which distinct emission from the direct and indirect gaps can be observed.

Finally, a detailed study of *p-i-n* photodiodes was conducted using quasi-Ge films doped with 0.05% ($\sim 1 \times 10^{19}$ cm^{-3}) Sn. The device measurements show current−voltage (*IV*) characteristics comparable to those of pure Ge analogues with similar geometry and thickness, suggesting minimal levels of deleterious defects in the active quasi-Ge component. More importantly, the magnitude of the spectral response of the quasi Ge was found to be more than two times higher than that of pure Ge on Si layers. Collectively, the device results demonstrate a marked improvement in the optoelectronic performance of quasi-Ge on Si, relative to pure Ge on Si.

II. FILM GROWTH

The formation of undoped quasi-Ge films was conducted directly on high resistivity Si(100) wafers via reactions of digermane (Ge_2H_6) and deuterated stannane (SnD_4) diluted by large amounts of high-purity H_2. The deposition experiments were performed at low temperatures of 390−400 °C and 0.300 Torr pressure using ultra high vacuum chemical vapor deposition (UHV CVD) methods and protocols similar to those described previously for the fabrication of dilute Sn alloys.[7] In the present work, the Sn concentration was also varied over a much more limited range of 10^{19} atoms per cm^3 (0.05%−0.15% Sn)—but controllably and reproducibly—by adjusting the amount of SnD_4 in the reaction chamber. Under optimized conditions, films with thicknesses up to 2 μm were produced at an average growth rate of 20 nm/min. We found that the growth rate did not increase monotonically as the SnD_4 content is further reduced in the digermane mixture (2%−3% by volume), but eventually began to decrease. In fact, the use of pure digermane did not produce any measurable film growth at the low temperatures and low pressures (0.3−0.4 Torr) employed. Accordingly, the use of a narrow processing window of temperature and SnD_4 flux is required in order to fabricate thick and atomically flat surfaces that are devoid of surface defects and imperfections over large lateral areas of at least 100 μm, as required for device applications. Using these procedures, the Stranski−Krastanov (SK) mechanism that typically defines the growth of Ge on mismatched Si surfaces is completely circumvented. The experiments suggest that a minimum critical concentration of SnD_4 is required at the growth front to ensure layer-by-layer crystal formation while maintaining unprecedented high growth rates at the low temperature employed.

The materials properties of the films were characterized by Rutherford backscattering (RBS), atomic force microscopy (AFM), Nomarski optical microscopy, cross-sectional transmission electron microscopy (XTEM), and X-ray diffraction (XRD). The data collectively indicate that the layer morphology and crystallinity are improved, compared to those of pure Ge films grown via our previously developed low-pressure CVD approach. The latter typically utilizes low-temperature reactions of Ge_2H_6, which is the main source of Ge, and trace amounts of $CH_2(GeH_3)_2$ metal−organic additives to produce device-quality materials with optical/electrical response similar or better than the state of the art.[8]

In the present study, initial examination of the samples using Nomarski microscopy showed that the layer surface was uniform, smooth, and featureless. Complementary AFM scans indicate a root-mean-square (rms) roughness of <1 nm for large areas in the range of 20 μm × 20 μm. XTEM micrographs confirm the flat surface morphology and indicate that the bulk material is devoid of threading defects within the typical field of view, as shown in Figure 1a for a representative film with a thickness of 1.2 μm. High-resolution images reveal the presence of quasi-periodic edge-type dislocations localized at the interface of the heterojunctions, as shown in Figure 1b. These defects are spaced ~8 nm apart and serve to fully absorb the differential strain between the substrate and the films. RBS analysis corroborates the XTEM-observed film thickness and, in some cases, reveals a weak Sn signal appearing slightly above the spectrum background, indicating that the dopant level is near the RBS detection limit of ~0.1%−0.15%, as shown in Figure 1c. Since the Sn content, in most samples, is below the RBS detection capability, we conducted routine SIMS analysis of all samples to determine the exact Sn content reliably and reproducibly. These SIMS data were calibrated using reference films containing 0% Sn (pure Ge) and 1.5% Sn, as measured by RBS. The SIMS study reveals a highly homogeneous Sn profile throughout the crystal at concentrations of $\sim 10^{19}$ atoms/cm^3.

High-resolution XRD measurements of the (224) and (004) Bragg peaks show that all materials are essentially strain-free "as-grown," regardless of their thickness (0.5−3 μm). This was a surprising outcome, since residual strains are very difficult to avoid in defect-engineered heteroepitaxy of highly mismatched materials. In particular, they are extremely common in Ge or $Ge_{1-y}Sn_y$ layers grown directly on Si(100) at 350−400 °C, thereby limiting the overall thicknesses that can be achieved. We find that the vanishing strain in the present case may be due to an optimal interplay between the Sn incorporation and the growth temperature, leading to facile integration of several micrometers and beyond film thicknesses. We have previously shown that an appropriate amount of Sn prevents island formation. The relatively higher temperature range accessible due to the low Sn content relieves local strain fields in the growth front. These favorable conditions ensure complete relaxation of the growing crystal from the very onset of layer formation, yielding atomically flat films with unprecedented thicknesses up to 3 μm at high growth rates up to 30 nm/min. The as-grown films exhibit relatively narrow (004) rocking curves with a typical full width at half-maximum (fwhm) of 800 arcsec, indicating a relatively low mosaic spread. This is significantly improved by rapid thermal annealing (RTA) processing at 680−725 °C for 10 s. The procedure markedly sharpens the XRD peak, leading to a reduction of the fwhm down to 200−150 arcsec. This value is lower than the best observed to date for the best Ge-on-Si samples. RBS ion channeling reveals a high degree of epitaxial alignment in the as-grown samples. This was significantly improved by subjecting the materials to RTA processing, as shown in Figure 1c, where final χ_{min} values are <8%.

Hall-effect measurements of the as-grown samples indicate that the material is *p*-type with background hole concentrations in the range of 2×10^{16} cm^{-3}. Intentional *n*-doping with P atoms was then conducted *in situ* using the single-source $P(GeH_3)_3$. This process yields tunable and highly controlled atomic profiles of the donor atoms. Carrier densities in the range of 1×10^{18} cm^{-3} to 2×10^{19} cm^{-3} were readily achieved by judiciously adjusting the $P(GeH_3)_3/Ge_2H_6$ ratio in the reaction mixture.

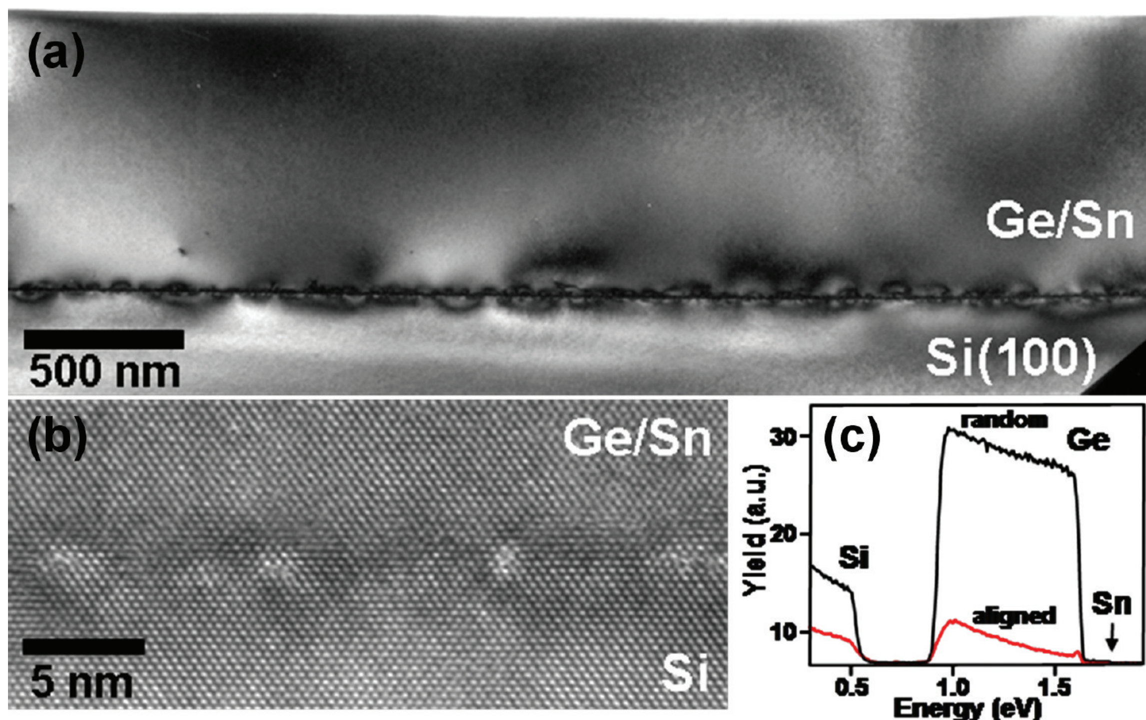

Figure 1. (a) XTEM image of "quasi-Ge"-on-Si film doped with 0.06% ($\sim 10^{19}$ cm^{-3}) of substitutional Sn. The area of the layer within the field of view is free of threading defects and exhibits a flat surface. (b) High-resolution image showing a periodic array of edge dislocations confined at the interface plane. (c) Random and channeled Rutherford backscattering (RBS) spectra of the same material. A weak Sn signal is observed confirming the presence of ~0.1% Sn% atoms. The high degree of channeling (red trace) indicates almost-perfect alignment between the film and the underlying Si(100).

The resultant layers exhibit flat surfaces, fully relaxed strain states, and crystallinity/morphology comparable to those observed in the intrinsic materials. However, the microstructure of heavily doped films near the 2×10^{19} cm^{-3} level also exhibits occasional isolated defects across the layer (see Figure 2). These seem to abruptly annihilate or terminate without further propagation through the crystal, and are presumably caused by the high concentration of P atoms. Despite these imperfections, the PL performance of these materials was far superior to that of undoped counterparts. All *n*-type samples were subjected to RTA treatments at 725 °C for 10 s, producing a significant improvement in the crystal quality and optical response. Under these conditions the active carrier concentration remained remarkably unchanged, indicating that no measurable out-diffusion of P atoms had occurred.

III. OPTICAL PROPERTIES

Photoluminescence (PL) is now routinely employed to assess the materials quality and device performance in a broad range of Ge-based semiconductor technologies. In fact, we have recently reported room-temperature PL in $Ge_{1-y}Sn_y$ alloys, as well as in pure Ge-on-Si films obtained via the low-pressure CVD method.[9] In this study, we demonstrate that similar PL spectra can be obtained from our quasi-Ge films. The PL experiments described here were performed using a 980-nm laser focused to a ~100-μm spot. The average incident power was 200 mW. The emitted light was analyzed with an f = 320 mm spectrometer equipped with a 600 lines/mm grating blazed at 2 μm, and detected with a single-channel, liquid nitrogen (LN_2)-cooled extended InGaAs receiver (1.3−2.3 μm range).

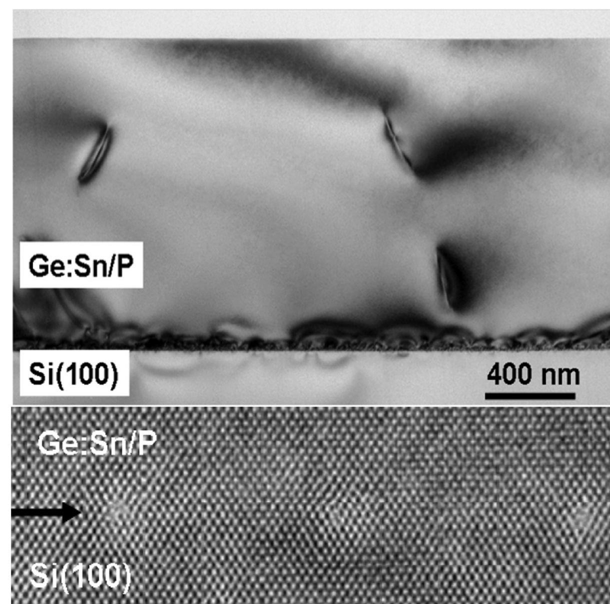

Figure 2. XTEM micrographs of a P- and Sn-co-doped film with impurity concentrations of 2×10^{19} cm^{-3} and 0.15%, respectively. The defects visible above the interface (top image) are attributed to the relatively high P incorporation. The micrograph also shows a high density of strain at the interface, caused by a periodic array of Lomer misfit dislocations marked by the arrow in the high-resolution image.

Figure 3 compares the PL signal from an annealed "quasi-Ge" film with the corresponding data from a reference Ge sample

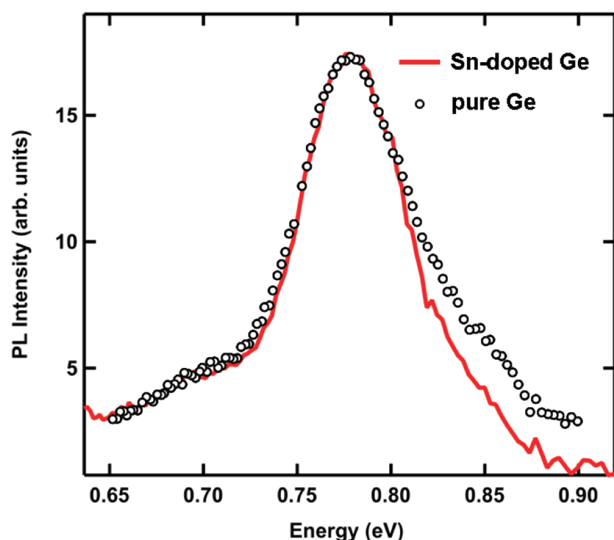

Figure 3. Room-temperature photoluminescence (PL) spectrum of a "quasi-Ge" sample (red trace), compared to a pure Ge film (circles). The maximum is assigned to direct-gap emission. The weak shoulder at lower energy corresponds to indirect-gap emission. The spectra are normalized to the same peak intensity.

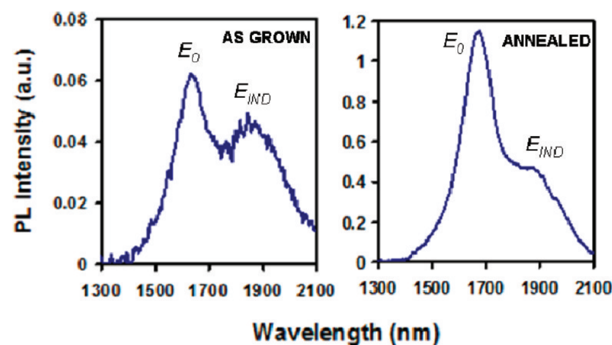

Figure 4. Room-temperature PL (left) of a fully relaxed, n-type quasi-Ge film with a thickness of 1200 nm and a carrier density of $\sim 2 \times 10^{19}$ cm^{-3}. Both the direct- and indirect-gap peaks are seen at 1635 and 1865 nm, respectively. The corresponding values for bulk Ge measured using the same procedure are found to be 1600 and 1795 nm. PL spectrum of the same Ge film (right) annealed at 725 °C. The overall emission intensity increases dramatically after annealing. The direct/indirect intensity ratio also changes as the thermal expansion induces a finite tensile strain in the film, as expected.

deposited via our low-pressure CVD process. We find that the peak position, which is assigned to the direct gap (E_0), is identical for both samples, confirming that the extremely small amount of Sn in the "quasi-Ge" material does not shift the emission wavelength or intensity. The low-energy shoulder, assigned to indirect gap transitions, is also virtually identical in both samples. On the high-energy side of the main peak, there is also a shoulder, similar to that observed in heavily p-type Ge and assigned to direct-gap transitions that do not conserve crystal momentum.[10] An alternative explanation, in our case, would be direct-gap emission from the Ge/Si interface, where a small amount of intermixing with Si might increase the direct-gap energy. Under any of these scenarios, it is apparent that the shoulder is weaker in the "quasi-Ge" sample, as might be expected for a higher-quality material.

Previous work of intrinsic Ge-on-Si with similar thickness (1−1.5 μm) has demonstrated that room-temperature PL is dominated by the direct-gap emission, as shown for our intrinsic materials in Figure 3.[11,12] This is in contrast to the PL behavior of bulk Ge, which is characterized by a strong but broad indirect peak (E_{ind}) and a much weaker direct gap shoulder (E_0). It has also been shown that n-doping at $(4-5) \times 10^{18}$ cm^{-3} in bulk Ge causes a measurable increase of the E_0 intensity, while the E_{ind} still remains the dominant feature. Any further increases of the direct-gap intensity in bulk Ge have thus far only been obtained by mechanically applying tensile strain in the range of 0.12%−0.37%.[13] In the case of Ge-on-Si, an increase in the direct-gap PL has been observed in doped and tensile-strained samples, but most previous studies do not cover the full spectral range corresponding to indirect-gap PL. Here, we extend the emission measurements down to 2100 nm to explore the indirect-gap emission in full detail. We find that this emission is also significantly enhanced via doping. As can be seen in Figure 4a, distinct direct and indirect peaks with comparable intensity are observed for a representative strain-free quasi-Ge sample with a thickness of 1200 nm and a carrier density of $\sim 2 \times 10^{19}$ cm^{-3}. To our knowledge, the PL in Figure 4a exhibits the strongest manifestation of the indirect gap observed thus far in thin-film materials. In particular, both E_0 and E_{ind} peaks are clearly resolved at 1635 and 1865 nm, with peak intensities that differ by less than ∼20%. It is important to note that the PL data shown in Figure 3 were obtained from samples that were subjected to RTA at 725 °C, while the as-grown counterparts did not show any measurable PL signal. This is in contrast to the observation of significant light emission from the n-type quasi-Ge shown in Figure 4a, and this is clearly a consequence of the relatively heavy doping, which introduces a sufficient carrier population at 2×10^{19} in the conduction band, as shown by a schematic of the Ge-like electronic structure in Figure 5.

The above observations suggest that both n-type doping and crystallinity improvement via annealing are responsible for the enhanced PL. To confirm this notion, we conducted a series of RTA experiments of the doped quasi-Ge samples. The principal outcome is that the highest PL intensity is obtained from samples annealed at 725 °C, as shown in Figure 4b. First, we see that the overall intensity increases by more than an order of magnitude, relative to the as-grown sample, as expected for improved crystallinity. Furthermore, the direct peak position shifts from 1635 nm to ∼1670 nm, and the direct/indirect PL intensity ratio also increases (the direct gap PL is ∼20 times more intense in the annealed sample), relative to the indirect PL (a detailed account of the shifts will be presented elsewhere). We have established via high-resolution XRD that a tensile strain of ∼0.18% is induced by the thermal treatment, while the as-grown sample is fully relaxed. This thermal strain contributes to the direct-gap emission shift as well as its relative enhancement. The tensile strain in the layers reduces the $L-\Gamma$ valley separation, shifting the Γ minimum toward the Fermi level and thereby enhancing the direct transition in the material (see Figure 5). This mechanism for light generation from Ge-like materials is reminiscent of the recently developed Ge-on-Si laser, in which the emission is achieved by optical pumping of n-type Ge structures that are both tensile strained at ∼0.20% and doped with phosphorus at levels of $\sim 1 \times 10^{19}$ atoms/cm^3.[14] In this regard, our quasi-Ge approach offers a low-cost, high-performance alternative to the above light source technology for applications in the 1550-nm telecom window (band).

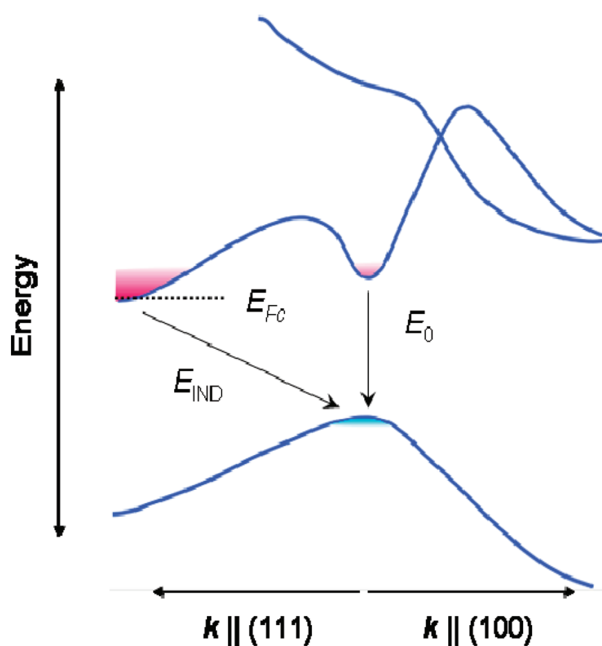

Figure 5. Schematic representation of the Ge band structure in the near-band-gap region. The arrows represent the transitions corresponding to direct (E_0) and indirect (E_{IND}) gap emission. E_{Fc} is the calculated position of the quasi-Fermi level in the conduction band for a doping concentration $n = 2 \times 10^{19}$. The shaded red and blue areas represent electrons and holes, respectively.

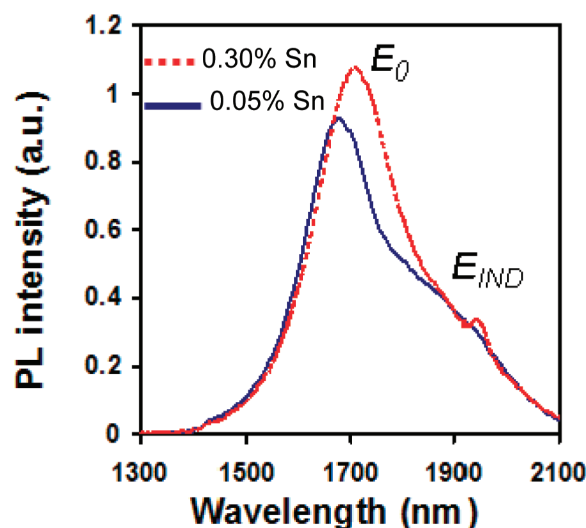

Figure 6. Room-temperature PL spectra of Ge-like films annealed at 725 °C and containing 0.05% (blue) and 0.3% Sn (red) doped with a fixed amount of P (2×10^{19} cm^{-3}). The peak intensity increases with Sn content and shifts to higher wavelengths.

The results thus far indicate that our synthesis approach affords a high level of control over the P and Sn contents (see ref 7). For example, for depositions conducted under identical conditions and with similar ratios of co-reactants, the P and Sn contents only varied by 1%−2%. Accordingly, here, we focus on independent variation of Sn content within the quasi-Ge compositional range while maintaining a fixed dopant level of P donors. Specifically, we investigate the PL performance of our quasi-Ge co-doped with the same P levels of 2×10^{19} (same as in the above samples) but with a slightly higher Sn concentration (in the vicinity of 0.3% or $\sim 1 \times 10^{20}$). The latter is at the upper limit of what we call quasi-Ge and is expected to yield a meaningful energy shift, relative to the highly diluted samples, whose PL peak positions are virtually indistinguishable to those pure Ge, as shown in Figure 3. As demonstrated above, the $\sim 2 \times 10^{19}$ donor levels are not only sufficiently high to enhance light emission, but they are also thermally robust to withstand RTA processing up to 725 °C without any significant diffusion of the P atoms from lattice sites, as typically observed under these conditions for samples with higher dopant concentrations. For example, activated P densities as high as $(0.7-1) \times 10^{20}$ cm^{-3} can be achieved in as-grown samples at 350 °C using our $P(GeH_3)_3$ process; however, these levels are invariably reduced down to a threshold of $(2-3) \times 10^{19}$ upon annealing at 650−725 °C. We note that similar levels of P concentration have been achieved by diffusion of P into Ge devices at similar temperatures.[15]

Atomically flat layers with the desired 0.3% Sn content were grown by appropriately adjusting the SnD_4 amount and were subsequently annealed at 725 °C to improve the crystallinity and enhance the emission intensity. SIMS profiles indicated that the average P and Sn contents of the "as-grown" material remained unchanged in the annealed counterparts (2×10^{19} and 0.3%, respectively). The Sn content was confirmed by RBS analysis, which showed a weak but distinctly visible Sn signal rising above the background of the measurement, indicating that the concentration is above the detection limit of ~0.1%, as expected. XRD on- and off-axis peaks were used to determine a residual tensile strain of 0.17%−0.19% in the annealed samples. As expected, the biaxial strain reduces the energy barrier between the lower indirect-gap valley and the direct-gap counterpart (Figure 5), resulting in a net increase of the electron population in the latter under similar external pumping conditions. Figure 6 shows the PL spectra acquired from samples containing different concentrations of Sn (0.3% (pink trace) and 0.05% (blue trace)) but the same amount of P (2×10^{19} cm^{-3}). Furthermore, since they undergo similar thermal treatments, they are found to possess a common tensile strain of 0.18%, as measured by XRD (see ref 16). In addition, the films have comparable thicknesses, in the range of 880−900 nm; therefore their PL intensities can be compared on equal footing. We notice that the main, direct-gap peak in the spectrum of the 0.30% Sn material is red-shifted and its intensity is slightly higher, relative to the 0.05% Sn counterpart. Both effects can be explained by the increase in Sn incorporation, which lowers the direct-gap energy and reduces its separation from the indirect gap, which leads to a larger electron population in the Γ valley (see Figure 5). This causes a stronger direct-gap emission. The reduction in the $\Gamma-L$ separation is apparent in Figure 6, where the peak maximum for the indirect-gap emission (broad shoulder-like features) is similar in both materials, whereas a clear energy downshift is observed for the direct emission.

For a final test of the quality of the quasi-Ge materials, we fabricated *n-i-p* diodes, incorporating layers containing 0.05% Sn and grown on highly *n*-doped 4-in. Si(100) wafers ($\rho = 0.003$ Ω cm). The diode typically consists of an ~850-nm-thick intrinsic film, followed by a 150-nm *p*-type capping overlayer. The latter was produced by adding appropriate amounts of diborane into the reaction mixture. After growth, the structures were subjected to three RTA cycles at 680 °C, for 10 s each.

 dx.doi.org/10.1021/cm201648x |*Chem. Mater.* 2011, 23, 4480–4486

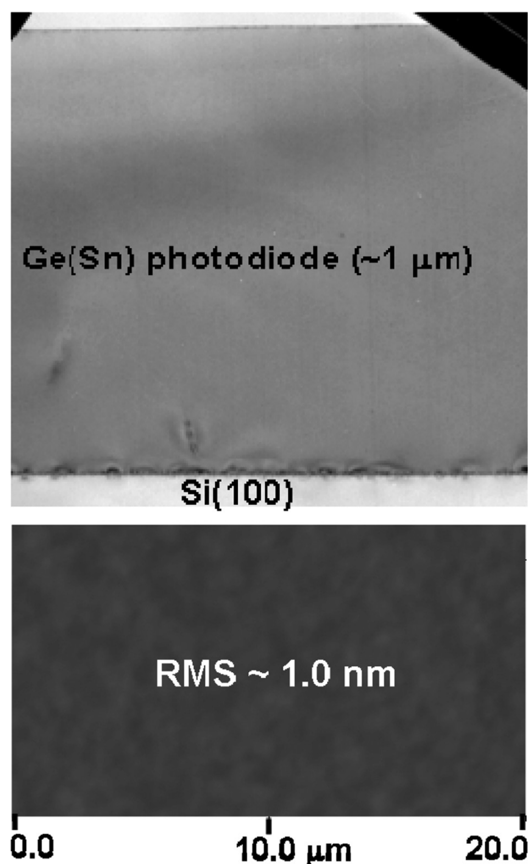

Figure 7. (Top) XTEM micrograph of the entire quasi-Ge photodiode structure (∼1 μm thick). The data reveal a virtually defect-free bulk layer and a perfectly smooth surface, indicating that no damage or degradation is caused to the devices by the various fabrication and processing steps. (Bottom) Corresponding AFM image of the material corroborating the flat surface morphology.

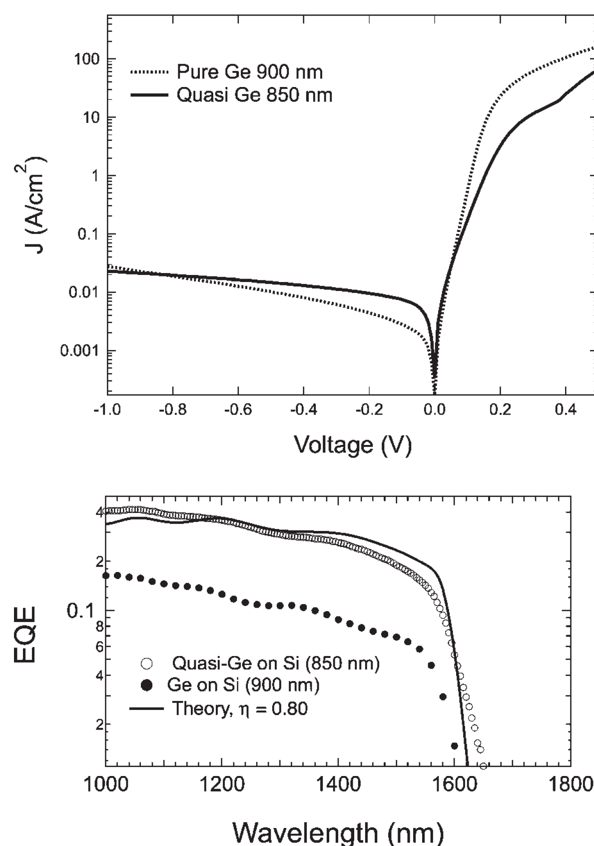

Figure 8. (Top) Current density versus voltage ($I-V$) graphs obtained from the Sn-doped Ge device and Ge reference samples. In both cases, the mesa sizes are ∼100 μm in diameter. (Bottom) External quantum efficiency (EQE) for a quasi-Ge heterostructure *p-i-n* diode measured at zero bias (empty circles), compared with a similar device based on pure Ge layers (full circles). The solid line is a theoretical curve that assumes a collection efficiency of η = 0.80 for the optically generated carriers.

Samples were processed using protocols similar to those used to fabricate $Ge_{0.98}Sn_{0.02}$ alloy photodiodes, described previously.[8] In this case, circular mesas with diameters ranging from 50 μm to 3000 μm were defined by photolithography and etched using reactive ion plasmas generated by BCl_3. The mesas were passivated by a 270-nm-thick SiO_2 layer, which also serves as antireflection coating. The Cr/Au metal contacts were deposited by e-beam and defined by lithography. Post processing XTEM investigations of the *p-i-n* devices reveal a near-perfect microstructure, suggesting that the relatively harsh fabrication steps do not cause any damage in the form of cracks, surface roughness, interface dislocations, and threading defects (see Figure 7). Atomic force microscopy (AFM) images of the same material indicated an rms roughness of ∼1 nm, indicating a flat surface morphology, which is consistent with the minimal level of defects detected by XTEM. These are highly encouraging results from the point of view of the reliability of our quasi-Ge-on-Si diode technology.

Current density versus voltage ($I-V$) measurements of the fabricated devices were conducted, and a representative curve for a typical 100-μm device is shown in Figure 8, where it is compared with the data measured from a Ge (900 nm) reference sample produced using our specialty low-pressure CVD ($\sim 10^{-4}$ Torr) approach.[5] Both curves exhibit a similar functional form, indicating clear rectifying behavior. Typical dark current density for the Sn-doped Ge device at −1 V bias is ∼0.02 A/cm^2, which is comparable to the 0.027 A/cm^2 value found in corresponding pure Ge devices grown on Si. These current density levels are consistent with high-quality material possessing threading defect densities of $<10^5$ $/cm^2$, as discussed in our previous work of Ge and GeSn-on-Si detector devices.[8] The low dark currents observed here are also consistent with a negligible degree of alloy scattering in these highly dilute alloys.

The spectral responsivity of the photodiodes, measured at zero bias, is plotted in Figure 8 and compared with corresponding data for a pure Ge reference device in *p-i-n* geometry. Both curves show a sharp decrease in the vicinity of ∼1600 and 1640 nm, respectively, corresponding to the direct-gap absorption edge. The 1600-nm value is almost identical to that measured in various *p-i-n* and *n-i-p* Ge photodiodes reported in the literature.[8] Both samples exhibit similarly high degrees of crystallinity, as evidenced by the fwhm of their 004 and 224 reflections in the XRD spectra. The Sn-doped material has a residual strain of 0.18%,compared to 0.1% in Ge. This strain accounts for the optical shift of ∼30 nm between the two devices. A theoretical calculation of the EQE using the model of ref 8 reveals that the collection efficiency at zero bias is $\eta \approx 80\%$ in the quasi-Ge diode, whereas the pure Ge diode had a collection efficiency of $\eta = 34\%$. The superior collection efficiency of the quasi-Ge diode

probably indicates a lower level of residual doping in the nominally intrinsic layer.

IV. CONCLUSIONS

We show that the incorporation of dopant levels of Sn into Ge-on-Si films at nominal levels of 0.05−0.15 is sufficient to completely suppress the traditional island-like growth mode (Stranski−Krastanov) and produce high-quality layers with flat surfaces and fully relaxed microstructures. Films with thicknesses up to 5 μm are commonly produced at high growth rates (up to 30 nm/min), suggesting that this batch wafer process may represent a scalable, high-volume, and high-throughput CVD method for producing Ge-based materials for applications in photonics, including photovoltaics. We have also demonstrated that these films can be systematically co-doped with P atoms at controlled levels of up to 2×10^{19} cm^{-3}, and this allows tuning of the photoluminenscence (PL) profile, with respect to direct and indirect transitions, for the first time. Optimizations of the film quality using a single rapid thermal annealing (RTA) step and the precise control of doping levels and Sn content have produced unprecedented PL intensities for this class of thin-film materials, suggesting that applications in emitters akin to the reported Ge-on-Si laser are within reach. Furthermore, the fabrication of high-performance photodiode prototypes opens the door to applications in infrared (IR) telecom detectors. In this regard, our quasi-Ge approach offers a low-cost, high-performance alternative or complement to the above light source technologies for applications in the 1550-nm telecom window.

■ AUTHOR INFORMATION

Corresponding Author
*E-mail: jkouvetakis@asu.edu.

■ ACKNOWLEDGMENT

This work was supported by the U.S. Air Force (under Contract No. DOD AFOSR FA9550-06-01-0442) (MURI program), the Department of Energy (under Contract No. DE-FG36-08GO18003), and the National Science Foundation (under Grant No. DMR-0907600). We thank Dr. Tolle for assistance with TEM analysis.

■ REFERENCES

(1) Luryi, S.; Kastalsky, A.; Bean, J. C. *IEEE Trans. Electron Devices* **1984**, *31*, 1135–1139.
(2) Currie, M. T.; Samavedam, S. B.; Langdo, T. A.; Leitz, C. W.; Fitzgerald, E. A. *Appl. Phys. Lett.* **1998**, *72*, 1718–1720.
(3) Colace, L.; Masini, G.; Galluzzi, F.; Assanto, G.; Capellini, G.; Di Gaspare, L.; Evangelisti, F. *Solid State Phenomena* **1997**, *54*, 55–58.
(4) Luan, H. C.; Wada, K.; Kimerling, L. C.; Masini, G.; Colace, L.; Assanto, G. *Opt. Mater.* **2001**, *17*, 71–73.
(5) Wistey, M. A.; Fang, Y. Y.; Tolle, J.; Chizmeshya, A. V. G.; Kouvetakis, J. *Appl. Phys. Lett.* **2007**, *90*, 082108.
(6) Bauer, M.; Taraci, J.; Tolle, J.; Chizmeshya, A. V. G.; Zollner, S.; Smith, D. J.; Menendez, J.; Hu, C.; Kouvetakis, J. *Appl. Phys. Lett.* **2002**, *81*, 2992–2994.
(7) Roucka, R.; Beeler, R.; Mathews, J.; Ryu, M-Y; Yeo, Y-K; Menéndez, J.; Kouvetakis, J. *J. Appl. Phys.* **2011**, *109*, 103115.
(8) Roucka, R.; Mathews, J.; Weng, C.; Beeler, R.; Tolle, J.; Menendez, J.; Kouvetakis, J. *IEEE J. Quantum Electron.* **2011**, *47*, 213–222.
(9) Mathews, J.; Beeler, R. T.; Tolle, J.; Xu, C.; Roucka, R.; Kouvetakis, J.; Menéndez, J. *Appl. Phys. Lett.* **2010**, *97*, 221912.
(10) Wagner, J.; Viña, L. *Phys. Rev. B* **1984**, *30*, 7030–7036.
(11) Sun, X.; Liu, J.; Kimerling, L. C.; Jurgen, J. *Appl. Phys. Lett.* **2009**, *95*, 011911.
(12) El Kurdi, M.; Kocinieski, T.; Ngo, T.-P; Boulmer, J.; Debarre, D.; Boucaud, P.; Damlencourt, J. F.; Kermarerec, O.; Bensahel, D. *Appl. Phys. Lett.* **2009**, *94*, 191107.
(13) Lan, H.-S.; Chan, S.-T.; Cheng, T.-H.; Chen, C.-Y.; Jan, S.-R.; Liu, C. W. *Appl. Phys. Lett.* **2011**, *98*, 101106.
(14) Liu, J.; Sun, X.; Camacho-Aguilera, R.; Kimerling, L. C.; Michel, J. *Opt. Lett.* **2010**, *35*, 679–681.
(15) Posthuma, N. E.; van der Heide, J.; Flamand, G.; Poortmans, J. *IEEE Trans. Electron Devices* **2007**, *54*, 1210–1216.
(16) Beeler, R.; Roucka, R.; Chizmeshya, A. V. G.; Kouvetakis, J.; Menendez, J. *Phys. Rev. B* **2011**, *84*, 035204-1–035204-8.